

## RESEARCH ARTICLE

# Parametric Analysis of Ferrofluid Line Contact Elastohydrodynamic Lubrication

Amir Torabi\*, Hamid Amini Rastabi

Department of Technology and Engineering, University of Shahrekord, Shahrekord, Iran

**ABSTRACT** – Ferrofluids are stable colloidal suspensions consisting of magnetic nanoparticles. A ferrofluid can be kept in a particular location by applying a suitable magnetic field. This feature is crucial in improving lubrication, especially in situations where there is a possibility of starvation. In this paper, a model for ferrofluid elastohydrodynamic lubrication is presented. Very detailed parameters of ferrofluid, such as magnetic saturation, ferrofluid radius, surfactant thickness, and ferrofluid concentration, are considered in this model. Then, various factors that affect the lubricant flow, such as load, entraining velocity, ferrofluid type, ferrofluid specification, and concentration on lubricant film thickness variation and friction coefficient, are investigated. The governing equations of ferrofluid flow, such as continuity, modified Reynolds equation, ferrofluid properties relationships, magnetic intensity, film thickness, and load equation, are derived and simultaneously solved in Matlab to find the pressure variation and local film thickness. The results show that by increasing the load, the particle size, and the volume concentration, the lubricant film thickness decreases, and the friction coefficient rises. Also, by increasing the speed, magnetic saturation, and magnetic field intensity, the thickness of the lubricant layer will increase, and the friction coefficient will decrease. At low loads, using ferrofluid will improve the friction coefficient by about 15% and at high loads by about 40%. The effect of ferrofluid at different speeds is about a 30% reduction in the friction coefficient. The optimum ferrofluid concentration was also estimated to be 2% by volume. Finally, the optimal state of using ferrofluid based on type, mixing percentage and coating thickness have been obtained.

## ARTICLE HISTORY

Received : 22<sup>nd</sup> May 2024  
 Revised : 06<sup>th</sup> Mar. 2025  
 Accepted : 22<sup>nd</sup> Apr. 2025  
 Published : 01<sup>st</sup> June 2025

## KEYWORDS

*Friction*  
*Ferrofluid*  
*Elastohydrodynamic*  
*Lubrication*  
*Magnetic Field*

## 1. INTRODUCTION

Ferrofluids are stable colloidal liquid mixtures made of ferromagnetic nanoparticles and carrier fluid. The fluid can be an ester, a diester, a hydrocarbon, water, etc. Ferrofluid is an innovative material that exhibits natural liquid behavior with superparamagnetic properties. Ferrofluids do not retain their magnetic property until they enter an external magnetic field, so they are classified as superparamagnets. Each magnetic particle in the solution is covered with a surfactant, which prevents coagulation. The chosen surfactant molecules interact with magnetic particles to avoid the formation of a strong monomolecular layer over the particles. This prevents the particle aggregation by Van der Waals forces [1].

Ferrofluids have garnered significant attention because of their unique chemical and physical properties. Since their introduction five decades ago, conventional engineering applications of ferrofluids include sealing, separation, dampers, inkjet printing, grinding, and more [2,3]. Lubrication represents a common application for ferrofluids. The main advantage of ferrofluids over conventional lubricants is that their position can be influenced by an external magnetic field while the fluid flows. Other advantages include reduced lubricant requirements, minimal leakage, and controlled fluid flow paths [4]. Furthermore, when exposed to an external magnetic field, the lubricant viscosity increases, thereby enhancing its load capacity. These factors have led to significant applications of ferrofluids in lubrication engineering, particularly in thrust bearings and short bearings [5-7]. Shah [8] demonstrated that ferrofluids could enable a bearing with two parallel plates to support loads and that incorporating these materials into conventional bearings boosts load capacity. Chao and Huang [9] discovered that using ferrofluids facilitates changes and improvements in the dynamic characteristics of hydrodynamic grooved journal bearings.

Various factors affecting ferrofluids' bearing under a magnetic field have been studied in numerous studies. Singh and Ahmad [10] considered the thermal effect on a porous sliding bearing, Patel and Deheri [11] considered the slip parameter for a transversely porous parallel plate sliding bearing, and Shimpi and Deheri [12] discussed how porosity, deformation, and roughness affect the bearings. Huang et al. [13] showed that the magnetic field intensity distribution has a considerable effect on the tribological characteristics of ferrofluids. Their experiments show that ferrofluids have a proper friction reduction in the presence of an external magnetic field compared to the base fluid. Patel et al. [14] attempted to investigate the effect of roughness and sliding speed on the performance of a ferrofluid porous sliding bearing. Laghrabli et al. [15] claimed that rotational viscosity, magnetization, and volume concentration of the ferromagnetic particles can control the static characteristics of finite journal bearings. Their results showed that by using ferrofluid, the pressure, load

\*CORRESPONDING AUTHOR | A. Torabi | ✉ [torabi@sku.ac.ir](mailto:torabi@sku.ac.ir)

capacity, attitude angle, and side leakage increase, and the friction coefficient decreases. A study by Huang et al. [16] investigates the tribological characteristics of ferromagnetic ferrofluids at starting motion and evaluates the formation of lubricant film, friction coefficient, and temperature effect. Zhao et al. [17] modeled the elastohydrodynamic ferrofluid-lubricated simple gears under a transient thermal condition. The transient film thickness, pressure distribution, and friction coefficient variation of contact were compared for various ferrofluids.

Shah and Shah [18] studied ferrofluid-lubricated long journal bearings using both the rotational and translational approaches of the journal. A uniform transverse magnetic field controls the ferrofluid, which significantly modifies bearing performance. Huang et al. [19] proposed a model for mineral-based ferrofluid lubrication by deriving the governing equations. The effects of magnetic particle size and bulk concentration on the kinetic properties and film hardness were examined. Finally, the impact of magnetic field intensity was discussed. Shah and Shah [20] derived the generalized ferrofluid-based lubrication equation based on the Sheliomis model. Atlassi et al. [21] investigated the effects of roughness orientation on the load capacity and squeeze time of ferrofluid-lubricated finite journal bearings. They show that using ferrofluid in the presence of transverse roughness is more beneficial than longitudinal roughness.

When the contact surface features a non-conformal geometry (the centers of curvature of the two surfaces are not on the same side of the contact line), a large load is applied to a small contact area, resulting in an increase in pressure at the contact area. Consequently, the surface undergoes elastic deformation. In such cases, the elastic deformation can be comparable to the film thickness of the lubricant, leading to this lubrication regime being termed elastohydrodynamic. As the lubricant enters the contact interface, it experiences increases in both pressure and dynamic viscosity. In elastohydrodynamic lubrication, several parameters, including surface hardness, non-conformality, and the relationship between viscosity variation, pressure and temperature, are of significant importance. This domain of ferrofluid lubrication has recently garnered attention; for instance, Vaziri et al. [22] investigated the performance of a conical hydrodynamic ferrofluid bearing through finite element analysis. They predicted and analyzed plug formation zones, which are hardly detectable at low shear rates. Liu et al. [23] studied the tribological features of a ferrofluid within a mixed lubrication condition. The mixed lubrication model is established by integrating the film thickness and the surface roughness model into the hydrodynamic lubrication model. This model can estimate the lubrication state change, the minimum film thickness, the asperity bearing rate, the boundary film failure rate, the friction coefficient, and the operational dynamics of fluid under various operating conditions. Azzala et al. [24] studied the elastic deformation of the surfaces on the characteristics of a journal ferrofluid bearing. The modified Reynolds equation was solved using the finite difference method to derive the pressure distribution. Their findings revealed that the inclusion of magnetic fields significantly enhances the performance of both rigid and deformable journal bearings.

In this research, a model for ferrofluid elastohydrodynamic lubricated contact is presented. At first, the governing equations and important relationships are extracted, and their discretization and solution methods are stated. According to the modeling presented in this research, the important parameters involved in ferrofluid lubrication between two nonconformal surfaces, such as applied load, surface speeds, ferrofluid type, magnetic field intensity, ferrofluid particle size, and their concentration, will be investigated.

## 2. GOVERNING EQUATION

Figure 1 shows the geometry of the lubricated contact surfaces. It is assumed that the linear contact between the pin and the disk is carried out inside a magnetic field created by a ferrofluid lubricant. The pin is fixed, and the disc is stirred with constant velocity. Fully flooded lubrication conditions are maintained. The fluid flow within the contact area of two bodies, while under the influence of the load applied between the two bodies, creates pressure in the lubricant layer. This pressure separates the two surfaces from each other. The presence of magnetic effects in the flow field and the influence of the magnetic fluid can help this lubrication process. It controls the path of fluid movement and makes the lubricant last longer between the two contact surfaces.

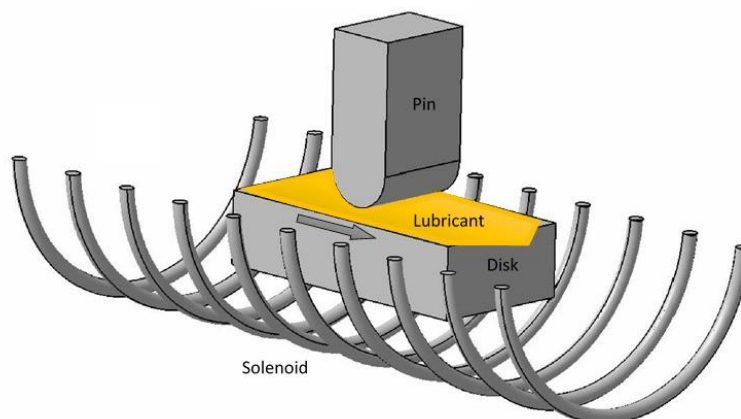


Figure 1. The study geometry

Therefore, there is a set of equations governing the problem that, considering the assumption of isothermality, these equations are separated into mass conservation, momentum conservation for fluid motion, fluid rheology equations, surface deformation equations under the influence of an applied load, equations related to calculating the force due to the magnetic field, and the load equation for balancing the pressure created in the lubricant layer. The governing equations, which are successively presented, should be solved simultaneously.

## 2.1 Reynolds Equation

The lubricant is assumed to flow in the  $x$  direction, and the distance between the two bodies is in the  $z$  direction. Since there is a thin lubricant layer, the pressure can be assumed to be uniform across this layer. The continuity equation can be written for the 2D velocity ( $u, v$ ) assumption of a magnetic fluid with a density of  $\rho_f$  as follows:

$$\frac{\partial \rho_f}{\partial t} + \frac{\partial(\rho_f u)}{\partial x} + \frac{\partial(\rho_f v)}{\partial y} = 0 \quad (1)$$

The momentum conservation equation of a ferrofluid under a magnetic field can be written as follows [16]:

$$\rho_f \frac{d\vec{v}}{dt} = \rho_f \vec{g} - \nabla \left[ P + \mu_0 \int_0^H \mathbf{M} d\mathbf{H} - \mu_0 \int_0^H \rho_f \frac{\partial \mathbf{M}}{\partial \rho_f} d\mathbf{H} \right] + \mu_0 \vec{M} \cdot \nabla \vec{H} + \eta_H \nabla^2 \vec{v} + \frac{1}{3} \eta_H \nabla (\nabla \cdot \vec{v}) + \frac{1}{2t_s} \nabla \times (\Omega - \omega) \quad (2)$$

where  $\eta_H$  is ferrofluid viscosity,  $\mu_0$  is vacuum permeability,  $M$  is magnetization,  $\mathbf{V}$  is velocity vector, and  $\mathbf{H}$  is magnetic field intensity. The first term on the right-hand side is the gravitational body forces, the second one is the pressure forces resulting from fluid pressure and magnetic effects, the third term is the magnetic body forces, and the next terms are the viscous forces and forces resulting from fluid rotation due to the magnetic field. Since the magnetic effects pressure can be ignored compared to the fluid pressure, the equation is simplified as follows:

$$\rho_f \frac{d\vec{v}}{dt} = \rho_f \vec{g} - \nabla P + \mu_0 \vec{M} \cdot \nabla \vec{H} + \eta_H \nabla^2 \vec{v} + \frac{1}{3} \eta_H \nabla (\nabla \cdot \vec{v}) + \frac{1}{2t_s} \nabla \times (\Omega - \omega) \quad (3)$$

where  $g$  is the gravitational acceleration vector,  $\Omega$  is the rotational angular velocity of the ferromagnetic particle, and  $\omega$  is the vortex angular velocity of the base fluid. The Brownian moment of momentum and rotational inertia of magnetic particles can be neglected. After ignoring the inertia and gravity forces and assuming that the magnetic vector of a ferrofluid is parallel to the magnetic field, the following equation can be written.

$$\nabla P = \mu_0 \vec{M} \cdot \nabla \vec{H} + \eta_H \nabla^2 \vec{v} + \frac{1}{3} \eta_H \nabla (\nabla \cdot \vec{v}) \quad (4)$$

When two sufficiently long, non-conformal surfaces are contacting each other in the presence of a lubricant, side leakage can be neglected. The side leakage effect on most contact areas does not make sense. This is called line contact elastohydrodynamic lubrication, and the pressure variation along the side direction can be ignored. The contact of roller bearings and gears is categorized as line contact. In this situation, by calculating the velocity components from the momentum conservation equation in the form of equation (4) and putting them in the continuity equation, equation (1), the ferrofluid modified Reynolds equation can be derived:

$$\frac{\partial}{\partial x} \left( \frac{\rho h^3}{\eta_H} \frac{\partial p}{\partial x} \right) = 12 \mathbf{u} \frac{\partial(\rho h)}{\partial x} + \mu_0 M_s \frac{\partial}{\partial x} \left( \frac{\rho h^3}{\eta_H} \frac{\partial H}{\partial x} \right) + \frac{\partial(\rho h)}{\partial t} \quad (5)$$

where  $h$  is the film thickness of the lubricant and  $M_s$  is the saturated magnetization.

## 2.2 Properties Equation

The Dawson-Higginson relationship for an arbitrary pressure and Temperature ( $p, T$ ) for density in ambient temperature ( $T_0$ ), i.e.,  $\rho_0$ , is used for the carrier fluid of ferrofluid and is presented by the following equation [25].

$$\rho_c = \rho_0 \left( 1 + \frac{c_1 p}{1 + c_2 p} - c_3 (T - T_0) \right) \quad (6)$$

where  $c_1 = 0.6 \times 10^{-9} Pa^{-1}$ ,  $c_2 = 1.7 \times 10^{-9} Pa^{-1}$ , and  $c_3 = 0.00065 K^{-1}$ .

The density of ferrofluids can be expressed as the following equation [26]:

$$\rho = (1 - \phi) \rho_c + \phi \rho_f \quad (7)$$

where  $\rho_c$  is carrier fluid density,  $\rho_f$  and  $\phi$  are the density and the volume concentration of the ferromagnetic particle, respectively. Viscosity has a key role in lubrication and has an important effect on film formation. The pressure increases drastically in an EHL contact, which causes an enhancement in the viscosity. Therefore, the pressure-viscosity correlation has to be considered in the EHL simulation. When a ferrofluid moves into the magnetic field, the magnetic moment amongst the magnetic particles holds them aligned. Then, the rotational velocity difference between the base fluid and the particles increases. As a result, the shear force of the solid and liquid phases increases. In a macroscopic view, this

increases the viscosity of the ferrofluid [27,28]. The ferrofluid's viscosity under magnetic field stimulation can be stated in the following equation [29].

$$\eta(p,T,H) = \left( 1 + 2.5 \left( 1 + \frac{\delta}{r_p} \right)^3 \phi - 1.55 \left( 1 + \frac{\delta}{r_p} \right)^6 \phi^2 + \frac{1.5k}{\phi + \frac{3k_B T}{2\pi r_p^3 \mu_0 (\mu_r - 1) H^2}} \right) \times \left\{ \eta_0 \exp \left\{ A_1 \left[ (1 + A_2 p)^{Z_0} (A_3 T - A_4)^{-S_0} - 1 \right] \right\} \right\} \quad (8)$$

where  $\delta$  is surfactant thickness, and  $r_p$  is the ferromagnetic particle radius. Also,

$$A_1 = \ln(\eta_0) + 9.67, A_2 = 5.1 \times 10^{-9} p_H, A_3 = T_0 / (T_0 - 138), A_4 = 138 / (T_0 - 138) \quad (9)$$

$$S_0 = \beta T_0 / (A_1 A_3), Z_0 = \alpha p_H / (A_1 A_2)$$

### 2.3 Magnetic Field Intensity Equation

The magnetic field around the current-carrying wire is considered a closed circular line. The intensity of the field on any circle (or any point in space) is indicated by H. It can be said that the amount of magnetic driving force that falls in each unit along the path of the field lines, or the force that enters the single pole N particle from the field. In this relation,  $\mu_0$  is the material's absolute permeability coefficient, and  $\mu_0$  shows the value of the diffusion coefficient in vacuum.

According to Bio-Savar's law, the intensity of magnetic induction in a point (x, y) can be calculated [30,31],

$$H = \frac{j}{2} \left[ (x + L) \ln \frac{R + \sqrt{R^2 + y^2 + (x+L)^2}}{r + \sqrt{r^2 + y^2 + (x+L)^2}} - (x - L) \ln \frac{R + \sqrt{R^2 + y^2 + (x-L)^2}}{r + \sqrt{r^2 + y^2 + (x-L)^2}} \right] \quad (10)$$

where  $j = NI / [2L(R - r)]$ .  $L$ ,  $R$ , and  $r$  are the half-length, outer and inner radius of the solenoid, respectively.  $N$  indicates the number of turns of the coil, and  $I$  is the current.

### 2.4 Film Thickness Equation

If the geometry is assumed to be similar to the contact of a long roller with an equivalent radius,  $R$ , and a flat surface, then the film thickness equation is only determined in the flow direction. Due to the non-conformal surface contact, very high pressures will be produced within the gap formed by the contacting surfaces. This pressure causes elastic deformation of the solid surface. This deformation appears in the equation with the expression  $\delta(x)$  [32].

$$h = h_0 + \frac{x^2}{2R} + \delta(x) \quad (11)$$

$$\delta(x) = \frac{-2}{\pi E'} \int_{x_{min}}^{x_{end}} p \ln(x - x')^2 dx' \quad (12)$$

where  $h_0$  is the undeformed surface's minimum film thickness and  $E'$  is the reduced modulus of elasticity.

### 2.5 Load Balance Equation

The pressure distribution, which can be found after solving the modified Reynolds equation, has to tolerate the applied normal load,  $W$ . This equation is used to modify the initial guess of the minimum film thickness. This equation can be expressed as follows:

$$W = b \int_{x_{min}}^{x_{end}} p dx \quad (13)$$

where  $b$  is the contact width.

## 3. SOLUTION ALGORITHM

The material properties, contact geometry, and magnetic field characteristics are model inputs. The solution domain is meshed uniformly, and the finite difference method is used to discretize the governing equations. The modified Reynolds equation (Eq. 5) has two unknown parameters that should be solved simultaneously. In the elastohydrodynamic problem, surface deflection is an important term in the film thickness equation, and it is related to the pressure distribution on the surface. Therefore, the solution should first make a convenient guess for the pressure distribution and then modify it. The fluid properties, especially the fluid viscosity, change drastically with the pressure, causing very large pressures and sudden changes in a small part of the solution field. It greatly affects the convergence of the solution, and an initial guess of the pressure is also very important to prevent divergence. The most reasonable guess mentioned in the articles is the Hertzian pressure distribution. This pressure distribution is formed when two bodies without lubrication exert a load on each other. After this initial guess, the lubricant properties and the surface deformation are calculated. Then, the lubricant layer thickness is determined by considering a proper initial guess for the minimum film thickness. An initial guess of the minimum thickness of the fluid layer can be effective in the convergence of the solution. The magnetic field intensity in each mesh point is calculated, and its derivative is determined to be used in the Reynolds equation. By determining the thickness of the lubricant layer, the modified Reynolds equation can be solved in terms of pressure. The solution obtained from this step is compared with the previous pressure distribution. If their difference is within the

tolerable range, the pressure distribution solution is obtained according to the initial guess of the thickness. The convergence criterion is defined as:

$$\frac{\sum_{i=1}^n |P_i^{new} - P_i^{old}|}{\sum_{i=1}^n P_i^{old}} < 10^{-5} \tag{14}$$

In this step, the normal load calculated by integration of the solution's pressure distribution is compared with the normal load entered from the input data according to the load equation (Eq. 13). If this equation is satisfied, the solution is complete. Otherwise, the minimum of the lubricant layer thickness is modified, and the modified Reynolds equation is resolved according to this modification. The convergence criterion is defined as:

$$W - \sum_{i=1}^n \left\{ \frac{(P_{i+1} - P_i)}{2} \times (X_{i+1} - X_i) \right\} < 10^{-3} \tag{15}$$

The flowchart of the solution algorithm is shown in Figure 2.

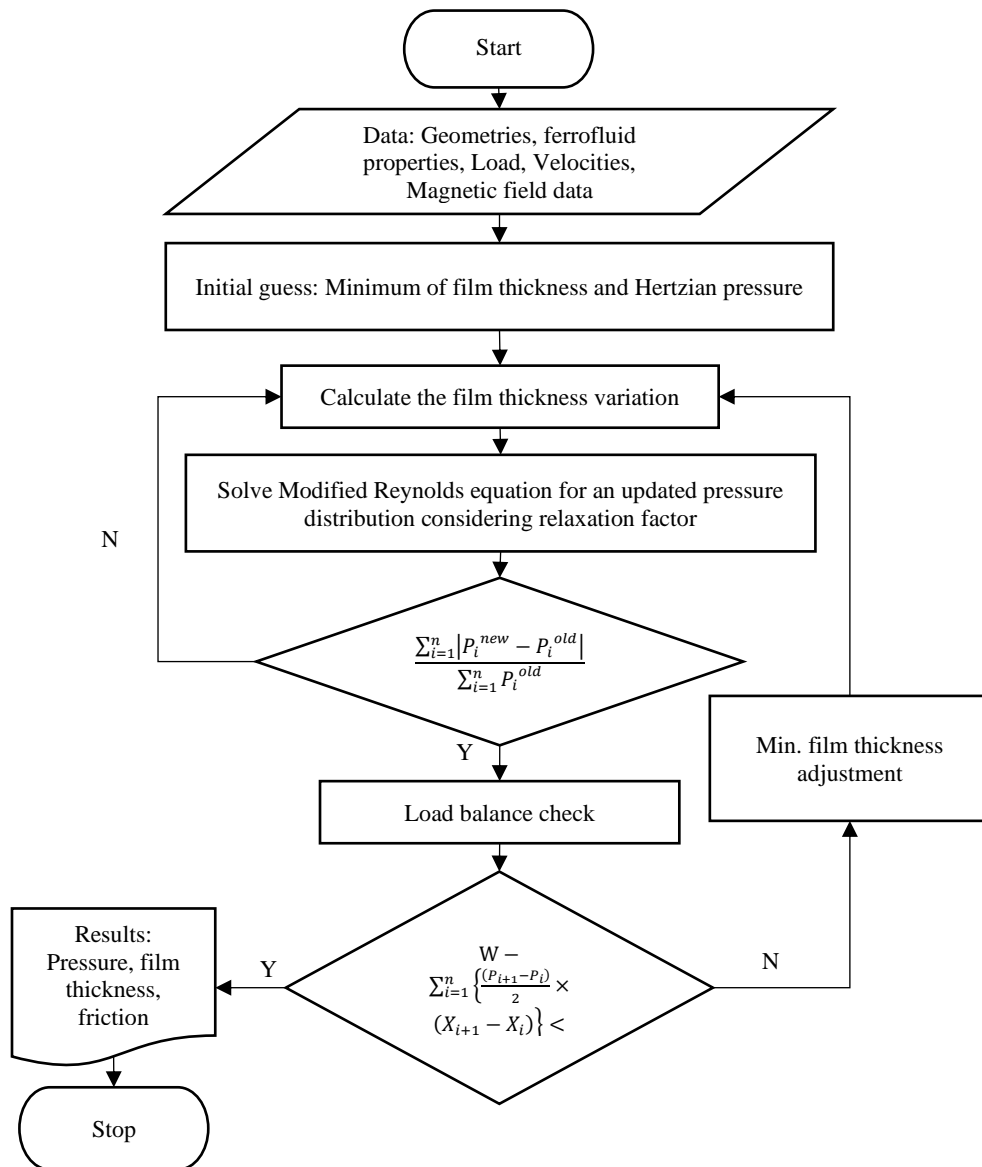


Figure 2. Solution algorithm

#### 4. RESULTS AND DISCUSSION

Ferromagnetic particles in a lubrication system can have both harmful and beneficial effects depending on how they are managed. When uncontrolled, these particles act as abrasives, increasing friction and wear on components such as bearings and gears, potentially leading to system failure. They can also clog filters, reduce lubricant flow, and promote corrosion. However, in a controlled context, their magnetic properties allow for efficient removal through magnetic filtration, improving system cleanliness. Additionally, monitoring the presence of ferromagnetic debris can serve as a valuable diagnostic tool for detecting early signs of wear, enabling predictive maintenance and extending equipment life.

Ghaednia et al. [33] observed the flow of lubricant through the contact area and perceived the formation mechanism of obstructed or plug flow. This flow reduces friction by allowing only a few layers of lubricant molecules to slide against one another. Small nanoparticles penetrate the very thin gaps between the in-contact surfaces, locally changing the characteristics of the lubrication process. The nanoparticles can alter the flow pattern of the contact area to further reduce friction. Singh et al. [34] reviewed the influence of nanoparticles on the lubrication system, statistically analyzing their effects. Various factors were studied regarding their impact on tribological performance. The most noticeable parameter was the size of the nanoparticles, which affects both friction and wear. The operating conditions and lubrication regimes are necessary for size optimization. Additionally, the morphology of the nanoparticles can affect friction, with onion and sheet-like morphologies outperforming others. The interaction between the nanoparticles and the environment determined the frictional performance.

Ferromagnetic lubrication systems are influenced by several key parameters that determine their performance and reliability. Particle size and shape affect how the particles interact with both surfaces and magnetic fields, with finer particles offering better suspension stability and larger ones enhancing magnetic response. The concentration of ferromagnetic particles plays a role in viscosity and lubrication efficiency, although excessive amounts can lead to sedimentation or increased wear. Magnetic field strength and orientation directly impact the behavior of magnetorheological lubricants by altering fluid properties in real time. The carrier fluid's viscosity, thermal stability, and compatibility are also crucial for maintaining particle suspension and system efficiency. Temperature influences both the fluid's and particles' behavior, potentially affecting magnetization and stability. Wear rate and surface roughness are important indicators of lubrication performance, while corrosion resistance is essential to prevent particle-induced damage. Ensuring dispersion stability helps maintain consistent lubrication, and sensor-based monitoring allows early detection of particle buildup or wear. Overall, tribological performance, including friction, load capacity, and anti-wear characteristics, depends on the careful balance of these parameters. In this section, various factors that affect the flow of the lubricating fluid between two surfaces are examined in relation to the lubrication parameters, such as the pressure distribution in the fluid, the thickness of the lubricating layer, and friction. According to the modeling presented in the third chapter, the important parameters involved in ferrofluid lubrication between two uneven surfaces are applied load, surface movement speed, ferrofluid type, magnetic field intensity, ferrofluid particle size, and composition percentage.

The minimum film thickness calculated for line and point contact modes is very close to each other [32, 33]. Therefore, this parameter is selected for comparison and validation. The present model is validated with a more complicated model introduced by Huang et al. [19]. The data was obtained at a normal load of 40 N and a current intensity of 1 ampere. As shown in Figure 3, at lower speeds, the error is close to 20%, but at higher velocities than 0.3 m/s, the error is less than 10%. This error can be reasonable in the point contact Huang model [19]. Since Huang's model [19] considered lateral leakage and was point contact, the difference between the results of the present model, which is linear contact, was predictable. Considering the point contact, with the increase in the speed of the surfaces, the lubricant entrance and its lateral leakage speed increase, and the overall fluid speed is higher in this case, and therefore the pressure is lower and, as a result, the thickness of the lubricant film is more predictable. At sufficiently low speeds, the pressures rise tremendously to balance the applied load, and therefore, the thickness of the lubricating layer drops a lot. In the case of linear contact, the one-dimensionality of the load balance with the applied pressure across the contact width provides more favorable situations for the formation of a slightly thicker layer. Wang et al. [35] reported similar results when comparing the linear and point contact minimum film thickness.

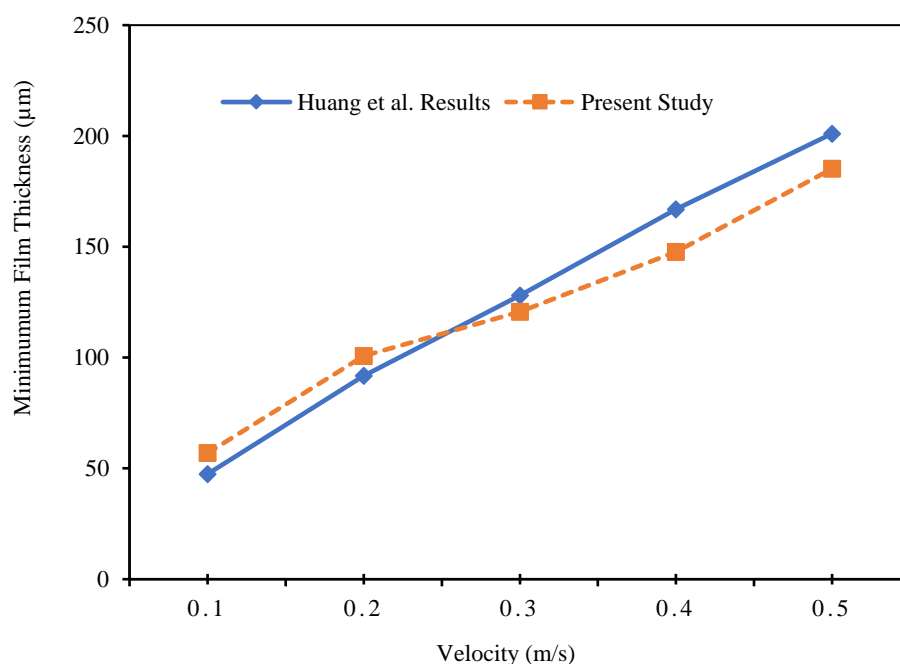


Figure 3. Concordance of the present model and Huang et al. [19] results

Table 1 lists the conditions of numerical calculation in the parameter study. These parameters are the same for all the simulations, and other operational parameters are changed in a wide range to investigate the effect of these parameters.

Table 1. Main parameters for all simulations

| Parameters | Values                                | Parameters | Values                          |
|------------|---------------------------------------|------------|---------------------------------|
| $\rho_0$   | 840 kg/m <sup>3</sup>                 | $E'$       | 211 GPa                         |
| $\eta_0$   | 0.02 Pa.s                             | $b$        | 0.02 m                          |
| $\alpha$   | $2.0 \times 10^{-8}$ Pa <sup>-1</sup> | $T_0$      | 298 K                           |
| $\beta$    | 0.045 K <sup>-1</sup>                 | $K_B$      | $1.3806505 \times 10^{-23}$ J/K |
| $R$        | 0.025 m                               |            |                                 |

#### 4.1 Load Effect

According to Figure 4(a), it can be revealed that with the increase of the load applied to the contact surface, the pressure formed in the fluid also surges. The pressure integral over the contact surface should be balanced with the applied load. Since the contact surface has limited changes in the range of 6 times the Hertzian contact half-width, this increase in load must be balanced by an increase in pressure. At low loads, the expansion of the pressure effect surface is enough to compensate for the load increase, but at higher loads, the entire pressure distribution will grow. The maximum pressure does not change up to a load of 40 N; after this, the maximum pressure increases by almost 90%.

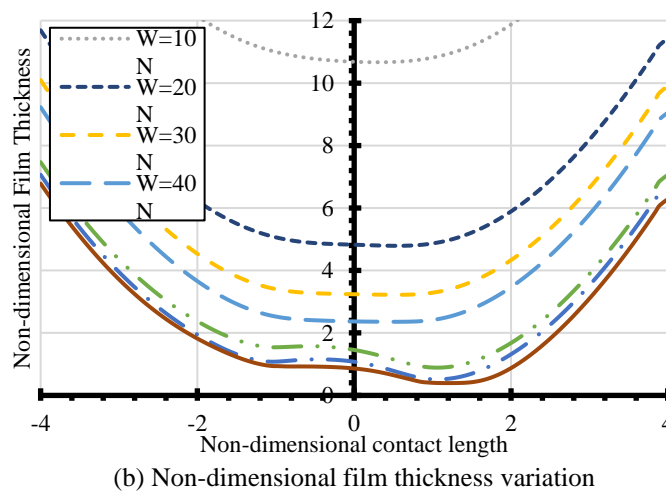
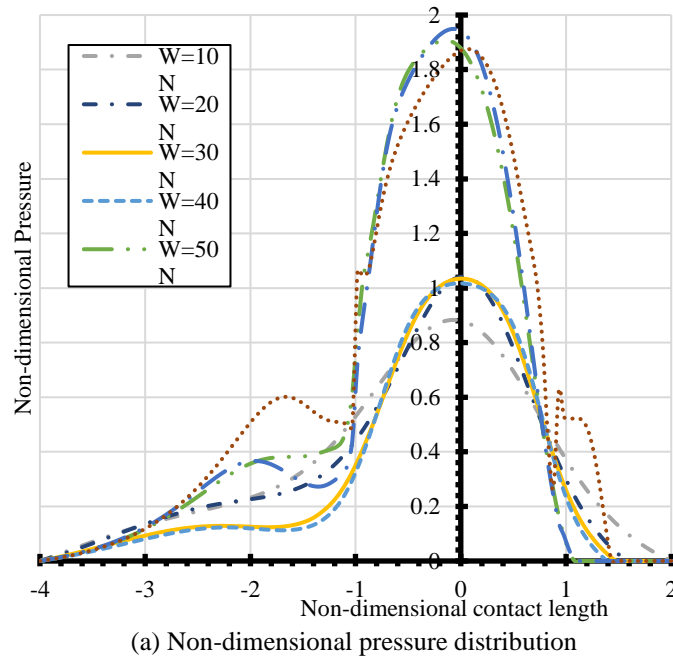


Figure 4. Non-dimensional pressure distribution and non-dimensional film thickness variation on the contact surface for different vertical loads

According to the results shown in Figure 4(b), as the applied load increases due to rising pressure, the thickness of the lubricant film decreases. When the load increases from 10 to 70 N, the minimum thickness of the lubricant film reduces by up to 25 times. The maximum reduction in the minimum thickness of the lubricant layer occurs at loads between 40 and 50 N, resulting in about a 2.5 times decrease. At loads exceeding 50 N, these changes diminish, and the minimum thickness of the lubricant layer alters more slowly. Under relatively high loads, significant surface deformation is observed due to high local pressure, with inward buckling noted at loads of 50 N and above. As the lubricant passes through the contact center and approaches the atmospheric pressure region, a process is carried out to prevent the fluid from escaping naturally. Consequently, a drastic reduction in thickness is observed at the outlet to reduce the flow rate.

In a light load, the pressure spike does not form. The film thickness becomes flat around the center of the contact area. When the load is high enough, i.e., more than 50 N, the pressure increases, and film thickness takes on a converging shape. At higher loads, a rapid change in pressure is finally observed, but it deviates from the typical characteristics of the elastohydrodynamic lubrication pressure profile. The magnetic term of the Reynolds equation serves as a fluid film formation mechanism, and it can reduce the pressure produced in the fluid film to a lower level.

As the load increases and the two surfaces compress against each other, resulting in a reduction of the lubricant layer, the velocity gradient increases, which signifies a larger shear stress. The friction force is calculated by integrating this stress over the contact surface. Therefore, as the load increases, so does the friction. As shown in Figure 5, the friction coefficient rises with the increased load. The use of ferrofluids compared to the base oil does not alter the rising trend of the friction coefficient, but the intensity of the increase with oil is much greater than that with ferrofluids. At light loads, the impact of ferrofluid is not very noticeable, but this effect becomes evident at medium and high loads. It appears that the presence of the magnetic field itself acts as a mechanism for lubrication.

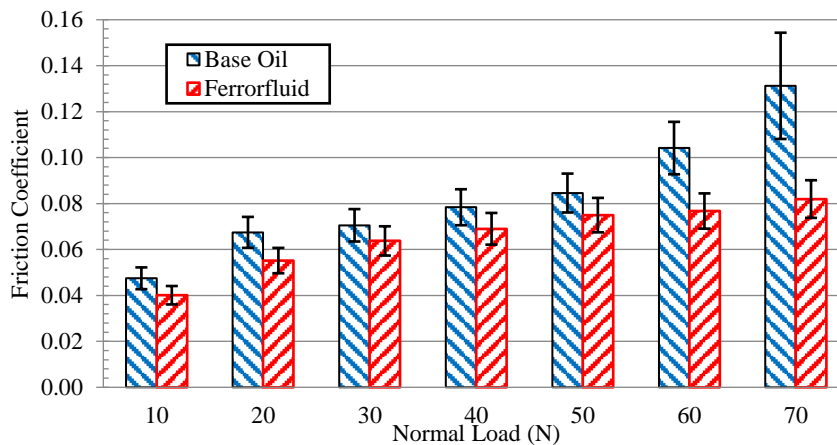


Figure 5. Base oil and ferrofluid friction coefficient comparison for different normal loads for constant condition:  $V = 0.1$  m/s,  $M_s = 95000$  A/m,  $I = 10$  A,  $\phi = 0.01$ ,  $r_p/\delta = 0.5$

## 4.2 Velocity Effect

As the speed of the surface increases, it results in greater shear stress. The friction force is calculated by integrating this stress over the contact area. Therefore, as the speed increases, the friction decreases. It can be seen in Figure 6 that the friction coefficient decreases with increasing speed, and friction also decreases. As expected, Ferrofluid has a positive effect in reducing the friction coefficient, but this effect is more obvious at low speeds.

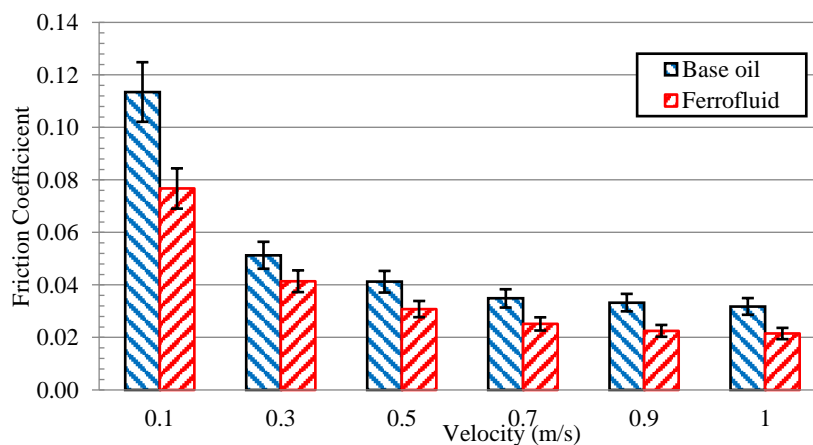


Figure 6. Comparison of friction coefficient variation for different velocities between ferrofluid and base oil for constant condition:  $W = 50$  N,  $M_s = 9500$  A/m,  $I = 10$  A,  $\phi = 0.01$ ,  $r_p/\delta = 0.5$

### 4.3 Ferrofluid Type Effect

Several types of ferrofluids are utilized in studies, differing mainly in magnetic saturation and particle size. The state where the magnetization of a magnet remains constant despite the amplification of the magnetic field is referred to as magnetic saturation. A higher magnetic saturation in a ferrofluid indicates an increase in the lubricant layer thickness, which results in lower viscous shear stress. Therefore, with greater magnetization saturation, friction decreases. It can be observed in Table 2 that increasing the magnetization saturation from  $1.5e4$  to  $9.5e4$  A/m results in a reduction of the friction coefficient by over 100 percent. The friction coefficient is closely related to magnetic saturation, showing a significant reduction once it exceeds  $7e4$  A/m. The magnetic saturation parameter can be particularly effective. An increase in this parameter enhances the second term on the left side of equation (5), which serves as a mechanism for bearing the contact load. Due to the non-linear relationship between pressure and the thickness of the lubricant layer, it is not possible to comment on the rate of change of these two based on this parameter, but a decrease can be anticipated with increasing magnetic saturation.

Ferrofluid particles are considered to be spherical magnetic material coated with a certain thickness of surfactant. The coating thickness to the sphere radius fraction is a key factor in the lubrication system performance. According to the results, with the increase in this ratio from 0.25 to 1.5, the lubricant layer thickness decreases, the minimum film thickness decreases by 65%, and the friction coefficient, as shown in Table 2, increases by 35%.

### 4.4 Magnetic Field Intensity Effect

As the intensity of the current entering the solenoid increases, the magnetic field becomes stronger, and the magnetic orientation increases. By increasing the intensity of the magnetic field, the lubricant layer thickness increases, and by increasing the electric current intensity passing through the solenoid from 1 to 20 A, the minimum film thickness of the lubricant layer increases up to 3 times. The maximum reduction in the minimum thickness of the lubricant film has been obtained at 20 A, which can be seen as up to a 100% increase. In the intensity of currents below 20 A, these changes are less, and the lubricant layer minimum thickness changes slowly. In the different current intensities, the surface severely deforms due to the high local pressure, and the inward buckling can be observed. This means that after passing through the contact center and returning the fluid to atmospheric pressure, a process is carried out to prevent the fluid from escaping naturally. Therefore, a drastic reduction in thickness is seen at the outlet to prevent fluid escape. As shown in Table 3, the friction coefficient decreases with the increase of magnetic field intensity, and when the current intensity changes from 1 to 20 A, the friction coefficient decreases by 40%.

Table 2. Friction coefficient variation for different ferrofluid types for constant conditions

| Load: 50 N<br>Entraining Velocity: 0.1 m/s<br>Current intensity: 10 A<br>Ferromagnetic particle concentration: 1%<br>Surfactant thickness per particle radius ratio: 0.5 |                      |           | Load: 50 N<br>Entraining Velocity: 0.1 m/s<br>Magnetic Saturation of Ferrofluid: 95000 A/m<br>Current intensity: 10 Amps<br>Ferromagnetic particle concentration: 1% |                      |            |
|--|----------------------|-----------|--|----------------------|------------|
| Magnetic saturation of ferrofluid (A/m)  | Friction Coefficient | Reduction | The ratio of surfactant thickness per particle radius  | Friction Coefficient | Difference |
| 15000  | 0.188                |           | 0.25   | 0.068                |            |
| 35000  | 0.161                | 13.96     | 0.50   | 0.076                | 12.50      |
| 55000  | 0.154                | 4.68      | 1.00   | 0.081                | 6.67       |
| 65000  | 0.150                | 2.59      | 1.30   | 0.084                | 3.13       |
| 70000  | 0.105                | 29.67     | 1.50   | 0.092                | 10.61      |
| 75000  | 0.087                | 17.64     |  |                      |            |
| 95000  | 0.076                | 12.26     |  |                      |            |

### 4.5 Ferromagnetic Particle Concentration Effect

Increasing the concentration of ferromagnetic particles alters the lubricant's viscosity and density. According to equation (8), this change occurs in such a way that viscosity increases with higher concentration. Greater viscosity enhances the thickness of the lubricant layer, but its effect on friction force can be somewhat different. An increase in viscosity leads to higher shear stress and friction force; however, an increase in the thickness of the lubricant layer results in reduced friction. The effect of thickness, particularly at a specific concentration of 2%, yields a reduction in friction. Yet, as concentration rises, the influence of the viscosity coefficient prevails, causing friction to increase. It is anticipated that increasing the volume concentration of ferromagnetic particles will elevate the pressure in the fluid. This pressure rises by 20% when the volume concentration shifts from 0.01 to 0.08. The minimum thickness of the lubricant layer diminishes by 82%. The greatest reduction in this minimum thickness is noted at a volume concentration of 0.08, where a reduction of up to 70% can be observed. As shown in Table 3, the friction coefficient escalates with increasing volume concentration of the ferrofluid; when this concentration changes from 0.01 to 0.08, the friction coefficient rises by more

than 100%. Notably, at a volume concentration of  $\phi = 0.02$ , there is an abrupt increase in the lubricant layer, which contradicts the prevailing trend. At this concentration, the coefficient of friction decreases due to the thicker lubricant layer.

Table 3. Friction coefficient variation for different ferromagnetic particle concentrations and current intensity

| Load: 50 N<br>Entraining Velocity: 0.1 m/s<br>Magnetic Saturation of Ferrofluid: 9500 A/m<br>Ferromagnetic particle concentration: 1%<br>Surfactant thickness per particle radius ratio: 0.5 |                      |           | Load: 50 N<br>Entraining Velocity: 0.1 m/s<br>Magnetic Saturation of Ferrofluid: 9500 A/m<br>Current intensity: 10 Amps<br>Surfactant thickness per particle radius ratio: 0.5 |                      |            |
|--|----------------------|-----------|--|----------------------|------------|
| Current intensity (Amps)   | Friction Coefficient | Reduction | ferromagnetic particle concentration (%)   | Friction Coefficient | Difference |
| 1  | 0.089                |           | 1  | 0.076                |            |
| 5  | 0.083                | 6.95      | 2  | 0.068                | -10.70     |
| 10   | 0.076                | 8.62      | 4  | 0.080                | 17.37      |
| 15   | 0.070                | 8.18      | 6  | 0.101                | 26.53      |
| 20   | 0.054                | 23.29     | 8  | 0.156                | 54.44      |

## 5. CONCLUSIONS

In this study, a detailed model for line contact elastohydrodynamic lubrication of a long cylinder and flat surface is developed. In ferrofluid lubrication, the existence of a magnetic field is considered as a lubrication mechanism along with the movement of surfaces. The magnetic effects cause changes in the pressure profile and lubricant film thickness in lubrication with ferrofluids. The pressure spike and the sudden decrease in thickness at the end of the contact zone are not seen for low loads. Compared to elastohydrodynamic lubrication with non-magnetic lubrication, a thicker film formation is expected in ferrofluids. Increasing the thickness of the lubricant layer means reducing friction. On the other hand, adding ferrofluid to the base fluid increases the viscosity of the final ferrofluid, which can cause an increase in friction. Therefore, the concentration of the ferrofluid and the type of magnetic particles used should be investigated.

The effect of various parameters on the friction coefficient of the elastohydrodynamic contact of ferromagnetic lubricant is investigated. These parameters are tribological conditions, ferrofluid properties, magnetic field characteristics, and nanoparticle concentration. The model outputs are pressure and film thickness distribution, which are used to calculate the friction coefficient. The following results are found:

- i) Increasing the load and reducing the entraining velocity increase the friction coefficient. Using the ferrofluid even in a weak magnetic field causes a notable reduction in the friction coefficient. The effect of ferrofluid in low entraining velocity and higher load is much more significant.
- ii) Ferrofluids have different magnetic saturations; the higher magnetic saturation causes a decrease in the friction coefficient. A sensible effect of this parameter is obtained when it reaches over 70000 and higher.
- iii) The size of the ferrofluid can affect the lubrication condition. The higher ratio of surfactant thickness to particle radius increases the friction coefficient. The fraction 0.25 can be a practical good choice.
- iv) The intensity of the magnetic field is an important factor when it reaches the effective range. Choosing 20 amperes for electric current intensity causes a sensible reduction in the friction coefficient.
- v) Particle concentration is a key factor in nanofluid application. Lower concentration causes a weak magnetic effect, while higher concentration increases viscosity and also the accumulation of particles in higher magnetic field intensity regions. Both can increase the friction coefficient, and there is an optimum concentration, which under the conditions of the problem, is calculated as 2 percent.

This study also has limitations, the most important of which is the assumption of line contact lubrication, isothermal fluid, and smooth surfaces. Each of these assumptions can be considered by adding effective parameters to the presented model, but this also makes the study more complicated and harder to solve. The model introduced in this study provides a balance between the level of complexity and the accuracy of the results.

## ACKNOWLEDGEMENTS

We are grateful for the invaluable support provided by the Engineering and Technology Department of Shahrekord University throughout the research process. The facilities and resources offered were extremely helpful and have been instrumental in completing this research project successfully.

## CONFLICT OF INTEREST

The authors certify that there is no actual or potential conflict of interest concerning this article.

## AUTHORS CONTRIBUTION

Amir Torabi (Conceptualization; Validation; Writing - draft; Supervision)

Hamid Amini Rastabi (Methodology; Investigation; Formal analysis; Software)

## REFERENCES

- [1] L. L. de Castro, C. C. Amorim, J. P. Miranda, T. D. Cassiano, and F. L. de Oliveira Paula, "The role of small separation interactions in ferrofluid structure," *Colloids and Surfaces A: Physicochemical and Engineering Aspects*, vol. 635, p. 128082, 2022.
- [2] M. Kole and S. Khandekar, "Engineering applications of ferrofluids: A review," *Journal of Magnetism and Magnetic Materials*, vol. 537, p. 168222, 2021.
- [3] M. D. Contreras-Mateus, A. Chaves-Guerrero, F.H. Sánchez, and N. N. Nassar, "Ferrofluids and magnetism in the oil industry: Theories, challenges, and current applications—A comprehensive review," *Physics of Fluids*, vol. 36, no.12, p. 121302, 2024.
- [4] X. Liu, W. Xu, H. Hu, Y. Wu, P. Yan, and B. Xu, "Parameter design and dynamic stability of controllable damping ferrofluid bearing," *Lubrication Science*, vol. 36, no.5, pp. 396-406, 2024.
- [5] J. Wen, Z. Anjum, Q. Dai, W. Huang, and X. Wang, "Controlling starvation of thrust ball bearing using magnetic fluids," *ASME Journal of Tribology*, vol. 147, no. 11, p. 114302, 2025.
- [6] K. Atlassi, M. Nabhani, and M. E. Khlifi, "Rotational viscosity effect on the stability of finite journal bearings lubricated by ferrofluids," *Journal of the Brazilian Society of Mechanical Sciences and Engineering*, vol. 43, no. 12, p. 548, 2021.
- [7] H. Rui, C. Hansheng, Z. Haoran, W. Humao, G. Junpeng, Y. Songshan, et al., "Research on magnetic fluid precise localized lubrication thrust cylindrical roller bearing with low-friction micro-vibration and high load-bearing capacity," *Journal of Physics: Conference Series*, vol. 2853, no. 1, p. 012016, 2024.
- [8] R. C. Shah and M. V. Bhat, "Lubrication of porous parallel plate slider bearing with slip velocity, material parameter and magnetic fluid," *Industrial Lubrication and Tribology*, vol. 57, no. 3, pp.103–106, 2005.
- [9] P. C. P. Chao and J. S. Huang, "Calculating rotor dynamic coefficients of a ferrofluid-lubricated and herringbone-grooved journal bearing via finite difference analysis," *Tribology Letters*, vol. 19, pp. 99–109, 2005.
- [10] J. P. Singh, and N. Ahmad, "Analysis of a porous-inclined slider bearing lubricated with magnetic fluid considering thermal effects with slip velocity," *Journal of the Brazilian Society of Mechanical Sciences and Engineering*, vol. 33, pp. 351-356, 2011.
- [11] N. D. Patel and G.M. Deheri, "Effect of surface roughness on the performance of a magnetic fluid based parallel plate porous slider bearing with slip velocity," *Journal of the Serbian Society for Computational Mechanics*, vol. 5, no. 1, pp. 104-118, 2011.
- [12] M. E. Shimpi and G. M. Deheri, "Effect of deformation in magnetic fluid based transversely rough short bearing," *Tribology-Materials, Surfaces & Interfaces*, vol. 6, no. 1, pp. 20-24, 2012.
- [13] W. Huang, C. Shen, X. L. Wang and S. Liao, "Study on the ferrofluid lubrication with an external magnetic field," *Tribology Letters*, vol. 41, pp. 145–151, 2011.
- [14] J. R. Patel, G. M. Deheri, and S. J. Patel, "Ferrofluid lubrication of a rough porous hyperbolic slider bearing with slip velocity," *Tribology in Industry*, vol. 36, no. 3, pp. 145–151, 2014.
- [15] S. Laghrabli, M. El Khlifi, M. Nabhani, and B. Bou-saïd, "Static characteristics of ferrofluid finite journal bearing considering rotational viscosity effect," *Lubrication Science*, vol. 29, no. 4, pp. 203–226, 2017.
- [16] X. I. Huang, X. Zhang, Y. O. Wang, "Numerical simulation of ferrofluid-lubricated rough elliptical contact with start-up motion," *Applied Mathematical Modelling*, vol. 91, pp. 232-260, 2020.
- [17] J.-J. Zhao, Y.-q. Wang, P. Zhang, and G.-x. Jian, "A Newtonian thermal elastohydrodynamic lubrication model for ferrofluid-lubricated involute spur gear pair," *Lubrication Science*, vol. 32, no. 2, pp. 33-45, 2020.
- [18] R. C. Shah and R. B. Shah, "Static and dynamic performances of ferrofluid lubricated long journal bearing," *Zeitschrift für Naturforschung*, vol. 76, no. 6, pp. 493-506, 2021.
- [19] X. I. Huang, W. Wang, L. I. Ding, and B. Yang, "Investigating the lubrication mechanism and stiffness of oil-based ferrofluids in spur gear drives," *Physics of Fluids*, vol. 33, p. 043103, 2021.
- [20] R. C. Shah and R. B. Shah, "Generalized ferrofluid based lubrication equation and its application to porous journal bearing," *ZAMM-Journal of Applied Mathematics and Mechanics*, vol. 102, p. e202000365, 2022.
- [21] K. Atlassi, M. Nabhani, and M. El Khlifi, "Ferrofluid squeeze film lubrication: surface roughness effect," *Industrial Lubrication and Tribology*, vol. 75, no. 1, pp. 133-142, 2023.
- [22] S. A. Vaziri, M. Norouzi, P. Akbarzadeh, M. Kim, and K. C. Kim, "Numerical analysis of conical hydrodynamic bearing lubricated with magnetorheological fluid," *Journal of the Brazilian Society of Mechanical Sciences and Engineering*, vol. 46, no. 2, p. 67, 2024.

- [23] Z. Liu, Z. Yan, S. Wu, H. Sun, and S. Zhang, "Experimental and numerical study of the mixed lubrication under the action of magnetic ionic liquid additives," *Scientific Reports*, vol. 14, no. 1, p. 5620, 2024.
- [24] A. Azzala, B. Chetti, and I. Zidane, "Numerical analysis of the effect of elastic deformation on the static characteristics of a circular journal bearing lubricated with a ferrofluid," *Proceedings of the Institution of Mechanical Engineers, Part J: Journal of Engineering Tribology*, vol. 239, no. 1, pp. 26-36, 2025.
- [25] D. Dowson and G. R. Higginson, *Elastohydrodynamic Lubrication, the Fundamentals of Roller and Gear Lubrication*, Oxford, Pergamon, 1966.
- [26] M. D. Cowley, "Ferrohydrodynamics," By R. E. Rosensweig, Cambridge University Press, p. 344, 1985. *Journal of Fluid Mechanics*, vol. 200, pp. 597-599, 1989.
- [27] A. Fang, "Consistent hydrodynamics of ferrofluids," *Physics of Fluids*, vol. 34, no. 1, p. 013319, 2022.
- [28] W. Yang, *Non-Equilibrium Ferrohydrodynamics*, CRC Press, 2025.
- [29] Z. Ren, Y. Han, R. Hong, J. Ding, and H. Li, "On the viscosity of magnetic fluid with low and moderate solid fraction," *Particuology*, vol. 6, no. 3, pp. 191-198, 2008.
- [30] P. Martín-Luna, B. Gimeno, D. González-Iglesias, D. Esperante, C. Blanch, N. Fuster-Martinez, et al., "On the magnetic field of a finite solenoid," *IEEE Transactions on Magnetics*, vol. 59, no. 4, pp. 1-6, 2023.
- [31] Q. G. Lin, "An approach to the magnetic field of a finite solenoid with a circular cross-section," *European Journal of Physics*, vol. 42, no. 3, p. 035206, 2021.
- [32] R. Manglik, *Engineering Tribology*, EduGorilla Publication, 2024.
- [33] H. Ghaednia, H. Babaei, R. L. Jackson, M. J. Bozack, and J. M. Khodadadi, "The effect of nanoparticles on thin film elastohydrodynamic lubrication," *Applied Physics Letters*, vol. 103, no. 26, p. 263111, 2013.
- [34] A. P. Singh, R. K. Dwivedi, and A. Suhane, "In the context of nano lubrication, do nanoparticles exhibit favourable impacts on all tribo surfaces? A review," *Protection of Metals and Physical Chemistry of Surfaces*, vol. 58, no. 2, pp. 325-338, 2022.
- [35] G. Wang, W. Wang, Y. Zhang, J. Shen, J. Xu, and K. Liu, "A solution for mixed elastohydrodynamic lubrication modeling considering effects of solid particles and surface roughness," *Proceedings of the Institution of Mechanical Engineers, Part J: Journal of Engineering Tribology*, vol. 236, no. 11, pp. 2272-2282, 2022.

## NOMENCLATURE

|       |  |                    |   |
|-------|--|--------------------|---|
| b     | Contact length, m                                      | $t_s$              | Newton relaxation time, s                                   |
| $E'$  | Reduced elasticity modulus, Pa                         | T                  | Temperature, K  |
| g     | Gravitational acceleration, $m/s^2$                    | $T_0$              | Ambient temperature, K                                      |
| h     | Lubricant Film thickness, m                            | $\vec{V} = (u, v)$ | Velocity, m/s   |
| $h_0$ | Minimum film thickness, m                              | W                  | Load, N   |
| H     | magnetic field intensity, A/m                          | x                  | Length dimension, m   |
| I     | Coil current, A  | y                  | Width dimension, m  |
| j     | Excitation current, A                                  | $\delta$           | Surfactant thickness  |
| J     | Central moment of inertia of magnetic particles, $m^4$ | $\phi$             | Volume concentration of magnetic particles                  |
| k     | The Ferrofluid thermal conductivity, W/m.K             | $\rho$             | Density, $kg/m^3$   |
| $K_B$ | Boltzmann constant                                     | $\rho_0$           | Density in ambient temperature, $kg/m^3$                    |
| L     | Half length of the solenoid, m                         | $\rho_c$           | Carrier fluid density, $kg/m^3$                             |
| M     | Magnetization, Tesla                                   | $\rho_f$           | Ferrofluid density, $kg/m^3$                                |
| $M_s$ | Saturated magnetization, Tesla                         | $\mu_0$            | Vacuum Permeability ( $= 4\pi \times 10^{-7} N/A^2$ )       |
| N     | Number of turns of the coil                            | $\mu_r$            | Relative permeability                                       |
| p     | Pressure, Pa   | $\kappa$           | Proportionality coefficient                                 |
| r     | Inner radius of the solenoid, m                        | $\eta$             | Ferrofluid viscosity, Pa.s                                  |
| $r_p$ | Ferromagnetic particle radii, m                        | $\eta_0$           | Ferrofluid viscosity in ambient temperature, Pa.s           |
| R     | The outer radius of the solenoid, m                    | $\omega$           | Vortex angular velocity of carrier fluid, rad/s             |
| t     | Time, s  | $\Omega$           | Rotational angular velocity of the magnetic particle, rad/s |